Revising the Basal Permittivity of the South Polar Layered Deposits of Mars With a Surficial Dust Cover

C. Grima, W. Kofman, A. Hérique, P. Beck

Geophysical Research Letters

RESEARCH LETTER
10.1029/2024GL109085

Revising the Basal Permittivity of the South Polar Layered Deposits of Mars With a Surficial Dust Cover

C. Grima[1,2], W. Kofman[3,4], A. Hérique[3], and P. Beck[3]

[1]Institute for Geophysics, The University of Texas at Austin, Austin, TX, USA, [2]Center for Planetary Systems and Habitability, The University of Texas at Austin, Austin, TX, USA, [3]University Grenoble Alpes, CNRS, CNES, IPAG, Grenoble, France, [4]Centrum Badan Kosmicznych Polskiej Akademii Nauk (CBK PAN), Warsaw, Poland

Abstract Bright basal reflections from the Mars Advanced Radar for Subsurface and Ionosphere Sounding (MARSIS) have been proposed to be consistent with permittivities characteristic of a wet material beneath the south polar layered deposits (SPLD). The characterization of a recently formed impact crater highlight the existence of a several meters thick ice-poor layer associated to a unit blanketing a large portion of the SPLD. We revise the radar propagation model used to invert the basal permittivity by including a surficial thin layer. We find that the inverted basal permittivity is highly sensitive to the properties of such a layer, with solutions ranging from common dry rocks to an unambiguously wet base. We advocate toward a better characterization of the surficial cover to assess the wet or dry nature for the base, and possibly reconcile most of the literature on the topic.

Plain Language Summary A localized bright radar reflection has been detected from the base of the Southern Martian polar cap. This reflection has been attributed to salty water infiltrating the material present beneath the ice. However, this result is not yet reconciled with other radar analyses and a debate has emerged on how liquid brine could be sustained at Martian conditions. Recently a 5-m thick layer of dust blanketing the surface of the ice cap has been detected from a recent crater excavation. This layer would act like a thin coating material that alters the apparent property of what is seen through a coated glass. At radar wavelengths, it can significantly modify the basal composition inferred from radar echoes. The bulk property of this layer is still unknown and a better characterization is necessary to inform the debate over a wet or dry base below the ice cap.

Key Points:

- We re-assess the radar inversion of the south polar layered deposits (SPLD) basal permittivity by incorporating the recently characterized dust layer mantling the ice
- The inverted basal permittivity is highly sensitive to the property of the surficial dust layer
- Better characterization of the dust layer is necessary in discriminating the nature of the SPLD bright basal reflector

Supporting Information:

Supporting Information may be found in the online version of this article.

Correspondence to:

C. Grima,
cyril.grima@utexas.edu

Citation:

Grima, C., Kofman, W., Hérique, A., & Beck, P. (2024). Revising the basal permittivity of the south polar layered deposits of Mars with a surficial dust cover. *Geophysical Research Letters*, *51*, e2024GL109085. https://doi.org/10.1029/2024GL109085

Received 1 MAR 2024
Accepted 3 JUN 2024

1. Introduction

Anomalous, isolated bright basal reflections have been detected at Planum Australe, beneath the south polar layered deposits (SPLD) of Mars by the Mars Advanced Radar for Subsurface and Ionosphere Sounding (MARSIS) onboard the Mars Express spacecraft (Lauro et al., 2020; Orosei et al., 2018). There, the normalized basal echo (Ψ), defined as the basal echo strength relative (P_{ss}) to the surface echo strength (P_s), reaches positive median values, that is, the buried interface is brighter than the surface. Under the assumption of signal propagation through a homogeneous vertical column of 205 K SPLD ice with 10% dust content, Orosei et al. (2018) derived a median real basal permittivity of 30, 33, 22 at 3, 4 and 5 MHz, respectively. The results at 4 MHz are usually those considered for further investigation because they derived from a more statistically representative set of measurements (Lauro et al., 2019, 2020; Orosei et al., 2018). Laboratory measurements and dielectric models indicate that such high permittivity on Mars could only be reached in a mixture including salty liquid water such as perchlorate brines (Mattei et al., 2022; Stillman et al., 2022). Frequency dispersion of Ψ between the 3, 4, and 5 MHz MARSIS frequency bands argue for a loss tangent of the ice higher than previously considered, leading to basal permittivity of ∼40 when attenuation is accounted for in the vertical propagation model (Lauro et al., 2022).

The hypothesis of a wet basal material at the SPLD is not reconciled with current understanding of polar geothermal state, however. Basal liquid water is thought to be unsustainable under the present-day Martian geothermal conditions, even with large amounts of salts that would depress the ice melting point (Sori & Bramson, 2019). The southern highlands are inferred to have a low geothermal heat flux (Broquet et al., 2021; Ojha et al., 2021) and thermophysical evolution modeling from the known composition of the SPLD does not predict conditions for sustainable basal liquid water to be reached.

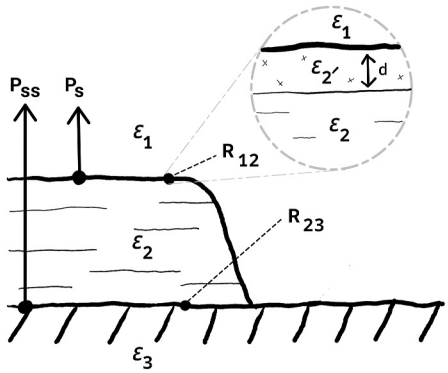

Figure 1. Considered structural setting. Subscripts 1, 2 and 3 refer to the atmosphere, the bulk south polar layered deposits (SPLD) ice and the SPLD bed, respectively. The subscript 2′ is for the mantling ice-poor unit of thickness d at the top of the SPLD.

All radar observations and analyses are not reconciled neither. Report of ubiquitous bright basal returns through the SPLD in contrast with the spatially confined early detection by Orosei et al. (2018), questions the sustainability of basal liquid water if it were to be maintained across such scales (Khuller & Plaut, 2021). A similar conceptual analysis from the 4-MHz reflection properties of the entire Martian surface, demonstrated that many currently exposed volcanic terrains would be as bright as the SPLD basal detection, if covered by a similar column of ice (Grima et al., 2022). An alternative hypothesis relevant to the current study proposed that a structural setting from alternations of thin layers of H_2O, CO_2 or possibly pure smectite, at the base of the SPLD could produce bright echoes through constructive interference of the radar signal (Lalich et al., 2021), although this was challenged by Orosei et al. (2022) for not reproducing the full range of observed Ψ. Recent advancements into the structure near the surface at Planum Australe suggest that a different vertical structure should be evaluated (M. Landis et al., 2024).

The bright basal reflector is located within the Aa2 geologic unit that extends over the largest portion of Planum Australe (Kolb & Tanaka, 2006). The profile and excavated material of two recently formed impact craters (<50 m diameter) in Aa2 suggest that a relatively ice-poor 5-m-thick layer covers a more ice-rich material (M. Landis et al., 2024). One of these craters (their crater B) lies about 160 km away from the bright basal reflector location. Its flat floor together with spotty and transient water ice detected in its ejecta, suggest that the 5-m excavation depth reached the transition to a lower ice-rich layer. The number of craters is not statistically representative, though, and the thickness lateral variations of this upper ice-poor layer is unknown. This layer is also consistent with the geologic interpretation of Aa2 mantling the more eroded topography of the bulk of the SPLD ice (Aa1) (Kolb & Tanaka, 2006). The widespread spatial extent of Aa2 strongly suggests that a several meters-thick ice-poor layer has to be taken into account by radar propagation models over the largest portion of the SPLD. Noteworthy, this relatively thick surficial layer is in contrast with in situ observations of a shallower ice table 5–18 cm deep at the Phoenix landing site in the Northern plains (P. H. Smith et al., 2009), implying climate events and/or depositional processes specific to Planum Australe.

In this study, we argue that the shallow transition from ice-poor to ice-rich material creates a coherent effect that lower the surface echo strength (Mouginot et al., 2009), therefore enhancing the normalized basal echo power. We take into account this Aa2 mantling unit into a 1-D vertical propagation model presented in Section 2. We then provide corresponding basal permittivity inversions for the Ψ measured by MARSIS in Section 3. We conclude in Section 4 with a discussion on how a spatially widespread thin slab of dust could reconcile most of the literature regarding the composition of the material at the bright basal reflector.

2. Model

The 1-D vertical structure we consider (Figure 1) can be seen as a generalization of the one considered by Orosei et al. (2020) for a homogeneous column of ice covering a base of unknown property, except that we also vary the Fresnel properties of the surface with the hypothesis of a thin slab at its top. The expression of Ψ is then identical to the one used by Orosei et al. (2020) to invert the basal permittivity at nadir incidence:

$$\Psi = \frac{P_{ss}}{P_s} = \frac{R_{23}}{R_{12}} T_{12}^2 A_2 \tag{1}$$

where the subscripts 1, 2 and 3 denote free space, the bulk SPLD ice and the base of the SPLD, respectively. A_2 is the 2-way signal attenuation in the ice given by $\exp(-2\pi f \tau \tan \delta_2)$ with f being the radar frequency, τ the one-way propagation time through the ice and $\tan \delta_2$ the loss tangent characterizing the ice electromagnetic absorption. Other variables in Equation 1 are the reflectance and transmittance at the surface (R_{12} and T_{12}, respectively), and the reflectance of the basal interface (R_{23}). An interface bounded by two half-infinite media of permittivity i and j has it reflectance and transmittance derived from the Fresnel coefficients (Ulaby, 2014):

$$R_{ij} = |r_{ij}|^2 = \left|\frac{\sqrt{\varepsilon}_i - \sqrt{\varepsilon}_j}{\sqrt{\varepsilon}_i + \sqrt{\varepsilon}_j}\right|^2$$
$$T_{ij} = \frac{\sqrt{\varepsilon}_j}{\sqrt{\varepsilon}_i}|t_{ij}|^2 = \frac{\sqrt{\varepsilon}_j}{\sqrt{\varepsilon}_i}\left|\frac{2\sqrt{\varepsilon}_i}{\sqrt{\varepsilon}_i + \sqrt{\varepsilon}_j}\right|^2 \quad (2)$$

In Orosei et al. (2018), the inversion of the basal permittivity ε_3 is done by using Equation 2 for R_{23}, then deriving ε_3 from the assessment of Equation 1 with a measured Ψ, and making assumptions for the bulk ice properties ε_2 and tan δ_2.

Let's consider now that the surface is blanketed by a non-absorbing slab of permittivity $\varepsilon_{2'}$ and with a thickness d on the order of the signal wavelength (λ). This scenario is known as a thin-film configuration. The corresponding effective Fresnel coefficients for such a surface can be derived from the Airy's formulation by summing coherently the amplitudes of successive reflections and refractions within the thin film (Yeh, 1998):

$$R_{12} = \left|\frac{r_{12'} + r_{2'2}e^{-2i\phi}}{1 + r_{12'}r_{2'2}e^{-2i\phi}}\right|^2 \quad \text{and} \quad T_{12} = \left|\frac{t_{12'}t_{2'2}e^{-i\phi}}{1 + r_{12'}r_{2'2}e^{-2i\phi}}\right|^2 \quad (3)$$

At normal incidence, the phase difference $\phi = 2\pi d\sqrt{\varepsilon_2}/\lambda$. The particular case of the standard Fresnel coefficients where there is no thin slab can be recovered from Equation 2 by setting $d = 0$ or $\varepsilon_{2'} = \varepsilon_2$. It is worth noting that Equation 2 satisfies the law of energy conservation $R + T = 1$, as obtained from the ratios of the Poynting power flows on each side of the surface to that of the incident wave. Substituting Equation 3 into Equation 1 allows evaluation of the various variables of our 1-D vertical model as a function of the thin slab properties at the top of the SPLD. The surface reflectance and transmittance are functions of the d/λ ratio, then varying through the MARSIS bandwidth of 1 MHz. Similar coherent (or resonant) effects have been reported from surficial and englacial layered structures at the North Polar layered deposits (NPLD) from multiband analysis of the 20-MHz Shallow Radar (SHARAD) data (B. A. Campbell & Morgan, 2018; Jawin et al., 2022; Jawin & Campbell, 2024). In the rest of this study R_{12} and T_{12} are convolved across the full 1-MHz MARSIS bandwidth with a synthetic linear chirp in the same way as in Mouginot et al. (2009) for analyzing the coherent effect on the 4-MHz MARSIS signal at the South residual CO_2 cap. Figure 2 illustrates the variation of the surface reflectance and transmittance for a range of thin slab property at MARSIS' 4-MHz band.

3. Application and Results

In this section, we invert a field of solutions for the basal permittivity ε_3 that matches the Ψ measured by MARSIS. We use the model described in Section 2 for a range of slab properties. Our approach is to feed our model with the parameters and assumptions used by Orosei et al. (2018) and Lauro et al. (2020) in deriving a basal permittivity of 33 at 4 MHz without a surficial slab, so that our results can be directly benchmarked against their, in the same way done by Grima et al. (2022).

MARSIS is a multi-frequency radar sounder on board the European Space Agency Mars Express spacecraft (Picardi et al., 2005). Its antenna transmits 1-MHz linearly chirped signals with a duration of 250 μs and centered at 1.8, 3, 4, and 5 MHz (167, 100, 75, and 60 m wavelength, respectively). Measurements for the median of Ψ at the bright reflector are not explicitly reported by Orosei et al. (2018) but can be recovered from digitization of their histograms in their figure S4. The cumulative sum of these histograms give $\Psi_{3MHz} = 2.1$ dB, $\Psi_{4MHz} = 2.5$ dB, $\Psi_{5MHz} = 0.8$ dB, indicating a basal return brighter than the surface. As noted by Orosei et al. (2022) Ψ also has excursions above 5 dB at 4 MHz, but not exceeding 10 dB. The same values are obtained by digitization of their Figure S5 in Supporting Information S1. The one-way propagation time in the ice is set to $\tau = 17$ μs to match observations (Lauro et al., 2020; Orosei et al., 2018). The relative permittivity used is $\varepsilon_2 = 3.4$ (Lauro et al., 2020), nearly corresponding to a bulk ice with a volumetric impurity rate of 10% (Plaut et al., 2007; Zuber et al., 2007), where the inclusions are derived from basaltic rocks. A loss tangent value for the bulk ice can be recovered from injecting the above stated parameters into Equation 1, giving tan $\delta_2 = 0.0008$ at 4 MHz.

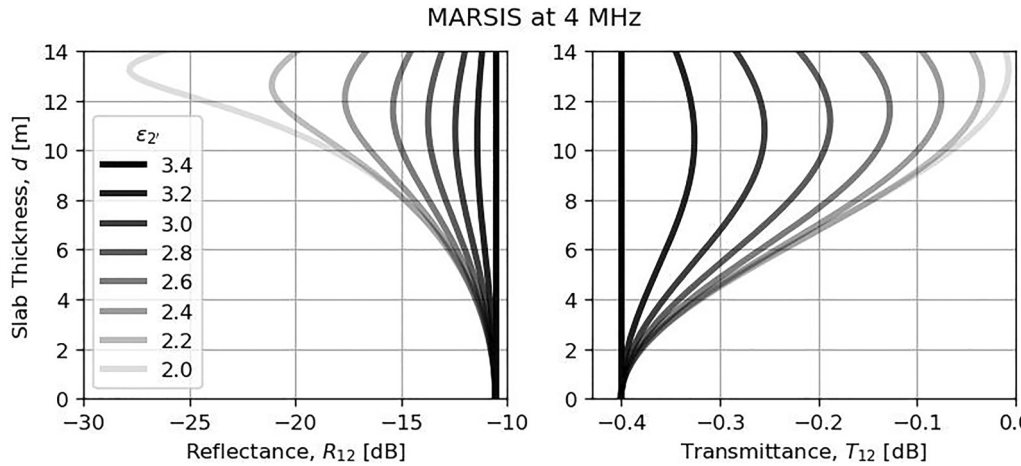

Figure 2. Surface reflectance and transmittance if overlaid by a thin slab of permittivity $\varepsilon_{2'}$ and thickness d at a 4-MHz center frequency with a 1-MHz bandwidth.

We now consider a thin slab mantling the surface. An indicative value for the thickness of the slab can be set to 5 m from the excavation depth at the site of crater B reported by M. Landis et al. (2024). This depth comes from one local measurement about 160 km away from the bright reflector, however, and in the absence of global understanding for its depositional and erosional mechanisms, spatial variations of this thickness is still unknown. The range of slab thickness can be upper-bounded by the Shallow Radar observations, though (Croci et al., 2011; Seu et al., 2007). SHARAD has an enhanced vertical resolution thanks to its 10 MHz bandwidth. To our knowledge, the SHARAD literature never reported the detection of a shallow interface that could be the base of the Aa2 ice-poor unit, suggesting its thickness is less than the SHARAD vertical resolution. The effective vertical resolution of a chirp radar sounder is obtained after range compression of the signal and is given by $\delta r = \alpha c/(2B\sqrt{\varepsilon})$, where c is the speed of light in vacuum, ε is the permittivity of the propagating medium, and α is an apodization factor arising from signal windowing for side lobe reduction, given to be $\alpha = 1.6$ for SHARAD (Seu et al., 2007). For a maximum $2 < \varepsilon_2' < 4$, the vertical range resolution ranges from 12 to 17 m.

Figure 3 presents all the Ψ values from our model at 4 MHz as a function of the slab properties. Curves for all the MARSIS frequency bands are also provided in Figure S1 in Supporting Information S1. While the initially measured median value of 2.5 dB can easily be reached in our model, we also observe that solutions exist for $\Psi > 5$ dB, a range corresponding to maximum values measured by Orosei et al. (2018). Figure 4 synthesizes the basal permittivity solutions that matches the Ψ measured by Orosei et al. (2018) at each MARSIS frequency, and as a function of the slab permittivity $\varepsilon_{2'}$ and thickness d. If the dust cover has a lower permittivity than the underlying ice, $\varepsilon_2' < \varepsilon_2$, then the basal permittivity is systematically lower than previously predicted and could lie in a wide range that starts as low as about 10 in the most favorable cases, a value that is more commonly found with dry geologic materials such as igneous rocks. Conversely, the basal permittivity would rapidly increase compared to previously predicted if the slab permittivity is greater than that of the bulk ice, a scenario that would strengthen the uniqueness of a wet base hypothesis. The property of the slab, is then essential in discriminating between the wet and the non-wet nature of the basal bright reflector.

The permittivity for an ice-poor regolith depends on its porosity and the permittivity of the dust grains. All are ultimately dependent on depositional, ablation and compaction processes that are still not well understood at the surface of the SPLD. for instance, Mie scattering modeling suggests that the lithic material deposited at the SPLD has a larger grain size than typical airfall dust found elsewhere on the Martian surface, suggesting processes preserving larger grains like aeolian erosion (M. Landis et al., 2024). As a possible analog, the dusty material at the surface of medusae fossae formation (MFF) on Mars is thought to be a friable weathering product with a permittivity estimated between 2 and 3 (B. A. Campbell, Watters, & Morgan, 2021). One can also attempt to define a broad range of regolith permittivity from other regolith properties gathered at Mars. Our investigation tool is the volume-based Looyenga dielectric mixing rule that defines the permittivity of a mixture of ε_a and ε_b as (Looyenga, 1965):

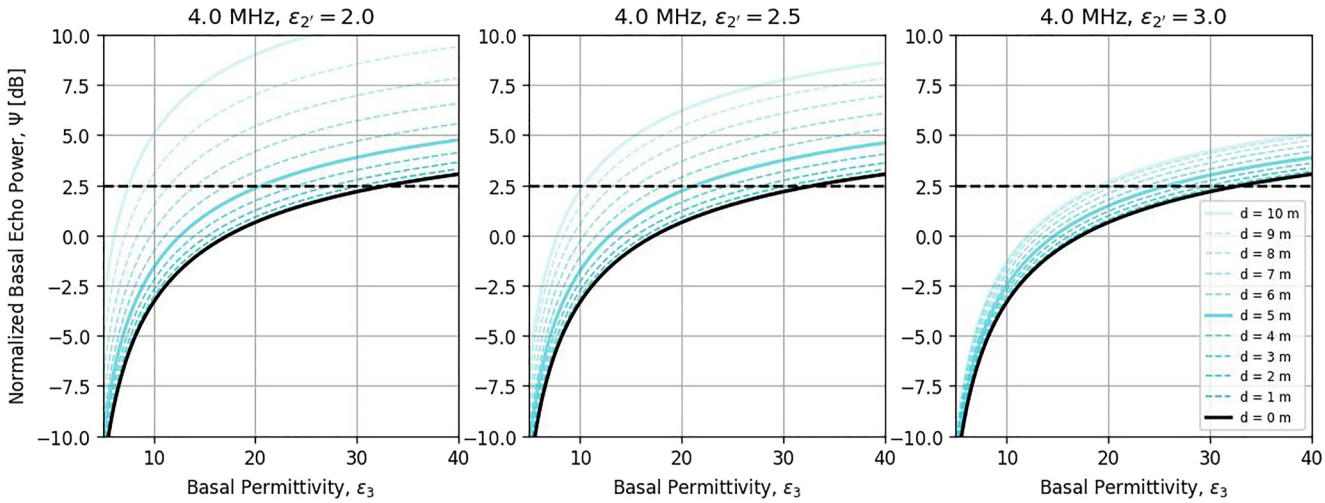

Figure 3. Expected Ψ for various set of basal apparent permittivity (ε_3) and slab properties (ε'_2, d) when the latter has a permittivity lower than the underlying bulk ice $\left(\varepsilon'_2 < \varepsilon_2\right)$. All results are convolved over a 1-MHz bandwidth with a 4-MHz center frequency. The black line is the no-slab solution. The horizontal dashed black line is the median Ψ measured by Orosei et al. (2018).

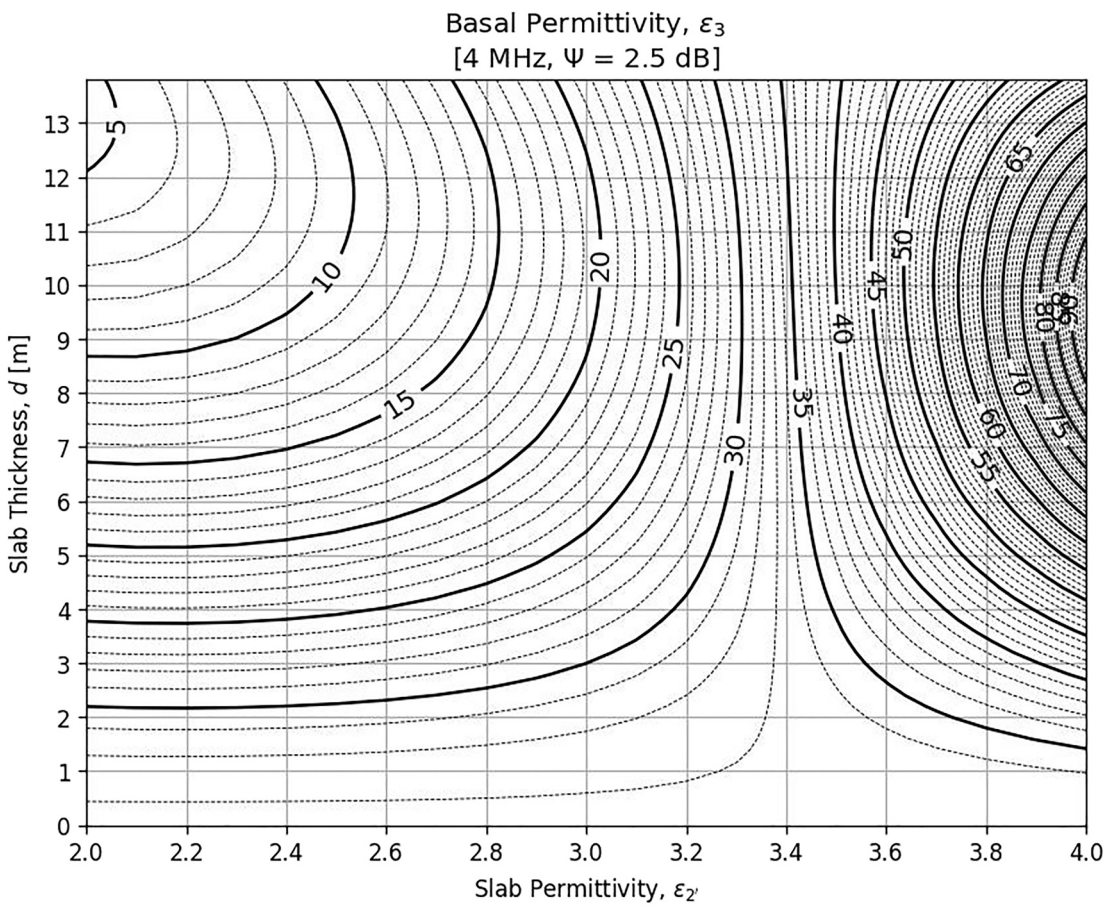

Figure 4. Basal permittivity as a function of the slab properties at 4 MHz for a reportedly measured median for Ψ of 2.5 dB, respectively. All results are convolved over a 1-MHz bandwidth. south polar layered deposits bulk ice is set to $\varepsilon_2 = 3.4$ and tan $\delta_2 = 0.0008$.

$$\varepsilon^{1/3} = \beta\left(\varepsilon_a^{1/3} - \varepsilon_b^{1/3}\right) + \varepsilon_b^{1/3} \quad (4)$$

where β is the volume fraction of ε_a in the total mixture. Then, the porosity of dry regolith as well as the permittivity of its dust grain are sufficient to assess the bulk regolith permittivity from Equation 4. They are, however, difficult to assess and might differ from standard Martian regolith as the mobilization process for the slab and its grain size appear different (M. Landis et al., 2024). The JSC Mars-1 simulant is a Martian regolith analog from weathered volcanic ash of the Pu'u Nene, a cinder cone on the Island of Hawaii. Its compacted and uncompact porosity is 44%–54%, respectively (Allen et al., 1997). Regolith found at the Viking 1 landing site has a bulk porosity of 60 ± 15% (Clark et al., 1977). Although the permittivity of the solid grains in the surface slab is unknown, it is common practice to consider the permittivity of basaltic materials for the lithic inclusions in the ice (Grima et al., 2022; Lauro et al., 2020; Orosei et al., 2018). We will do the same for the mantling slab by considering, on purpose, a broad range of typical values of 6–9 for that type of rocks (M. J. Campbell & Ulrichs, 1969; Rust et al., 1999; Telford et al., 1990), although outliers exist on both sides of the spectrum. Using Equation 4, a porosity of 44%, the bulk slab permittivity ε_2' would then lie between 3.1 and 4.1, while a 60% porosity would bring back those numbers between 2.3 and 2.9, standing in the range of permittivity (2–3) measured for the dusty material at the surface of the MFF (B. A. Campbell, Watters, & Morgan, 2021). These ranges of slab permittivity overlap ambiguously the one assumed for the SPLD bulk ice of 3.4. It does show, however that these properties are important to assess a correct basal permittivity and inform on its wet-versus-non-wet nature, eventually. Indeed, if the slab is assumed to be 5-m thick, as suggested by the excavation depth 160 km away reported by M. E. Landis and Whitten (2022), then the derived basal permittivity for $2 < \varepsilon_2' < 4.1$ could range approximately anywhere between 20 and 60, possibly approaching on its low-end dry mixtures of conductive minerals (Bierson et al., 2021; I. B. Smith et al., 2021; Stillman et al., 2022; Stillman & Olhoeft, 2008; Tulaczyk & Foley, 2020;). This range would change for a different slab thickness, reaching lower basal permittivities for a thicker slab. Standard basalts' permittivity up to 10 would require a slab as thick as 9 m in the best cases.

4. Discussions and Conclusions

We have integrated the recent characterization of an ice-poor dust cover (≤5-m thick layer mantling the SPLD) into the standard 1-D radar propagation model to invert the basal permittivity of the ice sheet from the normalized basal echo power Ψ where it has been measured by MARSIS as remarkably high (Orosei et al., 2018). The likely widespread spatial extent of this layer advocates for a more systematic integration into radar propagation models.

It stands out that whether the dust cover permittivity is higher or lower than the one for the underlying bulk ice might be a determinant question to discriminate between the wet and the dry hypotheses for the base of the SPLD at the location of the bright reflector. If $\varepsilon_{2'} > \varepsilon_2$, then the wet character of the base would be unambiguous as the permittivity quickly climbs closer to values characteristic of bulk liquid water ($\varepsilon \approx 80$ (Brouet et al., 2018)) that would be inaccessible to dry geologic materials, even at warmer Terrestrial temperatures. Conversely, $\varepsilon_{2'} < \varepsilon_2$ could lower the inverted basal permittivity toward materials more compatible with dry mixture of conductive materials (Bierson et al., 2021; I. B. Smith et al., 2021; Stillman et al., 2022; Stillman & Olhoeft, 2008; Tulaczyk & Foley, 2020). The thickness of the slab is also of importance. Although it is probably widespread across the SPLD, its thickness variations are unknown. The 5-m thickness estimated 160 km away from the bright basal reflector could gradually change over this spatial scale to reach values that would affect the basal permittivity inversion. For instance, a variation of ±2 m over that distance could have been unnoticed on the MARSIS surface reflectance (Figure 3), while it is able to vary the inverted basal permittivity by as much as 10 (e.g., from a value of $\varepsilon_3 = 15$ to $\varepsilon_3 = 25$) compared to the 5-m thick case. Note that a thicker layer would tend to increase the inverted basal permittivity for $\varepsilon_{2'} > \varepsilon_2$, while it would decrease it for $\varepsilon_{2'} < \varepsilon_2$.

The latter case of a layer permittivity lower than the SPLD ice would better reconcile the current conflicted literature, though. It has been observed that the MHz reflectivity property of currently exposed, yet dry, terrains at Mars are similar to that of the bright basal SPLD material (Grima et al., 2022). However, the initial $\varepsilon_3 = 33$ inverted by Orosei et al. (2018) appears to be likely related to exclusively wet matrices such as perchlorate brines (Mattei et al., 2022; Stillman et al., 2022). With a dust layer of relatively low permittivity mantling the SPLD, the basal permittivity would not be as high, reconciling Grima et al. (2022) and Stillman et al. (2022), but would also satisfy the growing literature indicating that the basal thermal conditions can hardly sustain liquid water

(Ojha et al., 2021, 2024). Lauro et al. (2022) uses the frequency dispersion of Ψ at 3, 4 and 5 MHz to derive a basal permittivity up to 40, higher than the initially 33 determined by Orosei et al. (2018). We suggest that the inversion by Lauro et al. (2022) is overestimated because all the frequency dispersion has been attributed to the attenuation in the bulk ice, while the reflection/transmission through the mantling slab should also be accounted as a component of the observed dispersion since it is highly frequency-dependent. Orosei et al. (2018) tested for the presence of a localized surficial CO_2-ice layer that could bias Ψ in the same way that we are assessing in this study. They argue that the relative spatial stability of the surface echo (P_s) beyond the sole location of the bright basal reflection demonstrates that there is no localized layering at the surface. However, the Aa2 unit associated with the dust layer is not local but widespread and ubiquitous across the whole region (Kolb & Tanaka, 2006). It is then reasonable to expect a spatially stable surface echo in the presence of this surficial dust cover. In this case, Ψ would be biased throughout much of the SPLD, thereby providing a mechanism that would also explain the observation by Khuller and Plaut (2021) of widespread high Ψ values across the SPLD.

A tighter characterization of the slab thickness and permittivity is then crucial to refine the radar propagation model and possibly discriminate between the wet and dry hypotheses for the base of the SPLD. This could be done with additional observations of recent impact craters to assess the lateral variability of the layer thickness, or with future radar sounders like the International Mars Ice Mapper (I-MIM) concept that would have a vertical resolution sufficient to image the slab (I-MIM MDT, 2022).

We acknowledge, however, that there are still many cases in Figure 4 where the slab properties might lead to ambiguous conclusions for the basal material. This is especially true if the inverted basal permittivity lies in the still being-investigated range of values valid for both wet and dry-conductive materials (Bierson et al., 2021; I. B. Smith et al., 2021; Stillman et al., 2022; Stillman & Olhoeft, 2008; Tulaczyk & Foley, 2020). However, our study integrates a growing body of work demonstrating that coherent effects from thin-layering have to be considered in propagation models (B. A. Campbell & Morgan, 2018; Jawin & Campbell, 2024; Lalich et al., 2022; Mouginot et al., 2009). One can imagine other coherent (resonant) effects from layering in the ice column and/or at the base to conjugate and further contribute to the measured Ψ. Especially, the possible impact of alternated H_2O and CO_2 ice basal layers as proposed by Lalich et al. (2022) should be reconsidered in complement to the existing surface dust cover assessed in our study. This could be done by letting R_{23} in Equation 1 be sensitive to thin layering as well.

A possible pervasive role of resonant and dispersive effects at the SPLD and at the NPLD is also supported by complex differential radiometric signatures between MARSIS and SHARAD, of which the effect of a thin surficial dust layer is only the last development. That includes different surface reflectivity between the SPLD and the NPLD (B. A. Campbell, Morgan, et al., 2021; Grima et al., 2012) where the latter is driven by a widespread, recent accumulated package also mantling the surface (Jawin & Campbell, 2024); The weakening of SPLD reflectivity at the location of the CO_2 residual polar cap (Mouginot et al., 2009); an extensive lack of SPLD basal and englacial echo (Whitten & Campbell, 2018) in SHARAD; the existence of a SHARAD diffused signal termed fog (Whitten & Campbell, 2018); the attested role of thin layering in the radiometric signature of englacial layers (B. A. Campbell & Morgan, 2018; Jawin et al., 2022; Lalich et al., 2019).

A better knowledge of the near-surface structure is also essential for a better absolute calibration of the MARSIS and the Shallow Radar (SHARAD). Mouginot et al. (2010) and Grima et al. (2012) calibrated the MARSIS and SHARAD signals, respectively, over a large reference zone that broadly encompass the location of the bright basal reflector and the impact crater where the dust layer has been characterized. Their assumption was that of a surface made solely of ice without surficial structure. The dust layer would change the effective reflection coefficient considered for calibration, then propagating to the permittivities derived for other Martian terrains. This sensitivity to calibration is discussed in more details in Grima et al. (2011) for SHARAD.

Data Availability Statement

Data were not used, nor created for this research.

Acknowledgments

We acknowledge the support of the space agencies of Italy (ASI) and the United States (NASA) for the development and science operations of MARSIS. Operations of the Mars Express spacecraft by the European Space Agency (ESA) are gratefully acknowledged. W.K. and A.H. acknowledge the French space agency (CNES) for supporting these studies in Institut de Planétologie et d'Astrophysique de Grenoble. C.G. is partially supported by NASA under award No 80NSSC23K1161. We thank Isaac Smith and an anonymous reviewer for their insightful comments. This is UTIG publication #3969 and CPSH publication #0074. This work is dedicated to the memory of our colleague and friend Jérémie Mouginot.

References

Allen, C. C., Morris, R. V., Lindstrom, D. J., Lindstrom, M. M., & Lockwood, J. P. (1997). JSC Mars-1: Martian regolith simulant. In *Lunar and planetary science conference* (p. 27).

Bierson, C. J., Tulaczyk, S., Courville, S. W., & Putzig, N. E. (2021). Strong MARSIS radar reflections from the base of Martian South Polar cap may be due to conductive ice or minerals. *Geophysical Research Letters*, *48*(13). e2021GL093880. https://doi.org/10.1029/2021gl093880

Broquet, A., Wieczorek, M. A., & Fa, W. (2021). The composition of the South Polar cap of Mars derived from orbital data. *Journal of Geophysical Research: Planets*, *126*(8). e2020JE006730. https://doi.org/10.1029/2020je006730

Brouet, Y., Neves, L., Sabouroux, P., Cerubini, R., Becerra, P., Grima, C., et al. (2018). Dielectric spectroscopy measurements of saline aqueous solutions in the VHF-UHF bands: Toward a dielectric model of icy satellite water reservoirs. In *5th IEEE international workshop on metrology for aerospace*.

Campbell, B. A., & Morgan, G. A. (2018). Fine-scale layering of Mars polar deposits and signatures of ice content in nonpolar material from multiband SHARAD data processing. *Geophysical Research Letters*, *45*(4), 1759–1766. https://doi.org/10.1002/2017GL075844

Campbell, B. A., Morgan, G. A., Bernardini, F., Putzig, N. E., Nunes, D. C., & Plaut, J. J. (2021). Calibration of Mars reconnaissance orbiter Shallow Radar (SHARAD) data for subsurface probing and surface reflectivity studies. *Icarus*, *360*, 114358. https://doi.org/10.1016/j.icarus.2021.114358

Campbell, B. A., Watters, T. R., & Morgan, G. A. (2021). Dielectric properties of the medusae fossae formation and implications for ice content. *Journal of Geophysical Research: Planets*, *126*(3). e2020JE006601. https://doi.org/10.1029/2020je006601

Campbell, M. J., & Ulrichs, J. (1969). Electrical properties of rocks and their significance for lunar radar observations. *Journal of Geophysical Research*, *74*(25), 5867–5881. https://doi.org/10.1029/jb074i025p05867

Clark, B. C., Baird, A. K., Rose, H. J., Toulmin, P., Christian, R. P., Kelliher, W. C., et al. (1977). The Viking X Ray fluorescence experiment: Analytical methods and early results. *Journal of Geophysical Research*, *82*(28), 4577–4594. https://doi.org/10.1029/js082i028p04577

Croci, R., Seu, R., Flamini, E., & Russo, E. (2011). The Shallow Radar (SHARAD) onboard the NASA MRO mission. *Proceedings of the IEEE*, *99*(5), 794–807. https://doi.org/10.1109/jproc.2010.2104130

Grima, C., Costard, F., Kofman, W., Saint Bézar, B., Servain, A., Rémy, F., et al. (2011). Large asymmetric polar scarps on Planum Australe, Mars: Characterization and evolution. *Icarus*, *212*(1), 96–109. https://doi.org/10.1016/j.icarus.2010.12.017

Grima, C., Kofman, W., Herique, A., Orosei, R., & Seu, R. (2012). Quantitative analysis of Mars surface radar reflectivity at 20MHz. *Icarus*, *220*(1), 84–99. https://doi.org/10.1016/j.icarus.2012.04.017

Grima, C., Mouginot, J., Kofman, W., Hérique, A., & Beck, P. (2022). The basal detectability of an ice-covered Mars by MARSIS. *Geophysical Research Letters*, *49*(2). e2021GL096518. https://doi.org/10.1029/2021GL096518

I-MIM MDT. (2022). *I-MIM MDT final report of the international Mars ice mapper reconnaissance* (Vol. 239). Science Measurement Definition Team.

Jawin, E. R., & Campbell, B. A. (2024). Recent widespread deposition in the Martian North and south polar layered deposits as revealed by multiband SHARAD surface reflectivity. *Journal of Geophysical Research: Planets*, *129*(3), e2023JE008082. https://doi.org/10.1029/2023je008082

Jawin, E. R., Campbell, B. A., Whitten, J. L., & Morgan, G. A. (2022). The lateral continuity and vertical arrangement of dust layers in the Martian north polar cap from SHARAD multiband data. *Geophysical Research Letters*, *49*(17), e2022GL099896. https://doi.org/10.1029/2022gl099896

Khuller, A. R., & Plaut, J. J. (2021). Characteristics of the basal interface of the Martian south polar layered deposits. *Geophysical Research Letters*, *48*(13), e2021GL093631. https://doi.org/10.1029/2021gl093631

Kolb, E. J., & Tanaka, K. L. (2006). Accumulation and erosion of south polar layered deposits in the Promethei Lingula region. *Planum Australe, Mars. MARS*, *2*, 1–9. https://doi.org/10.1555/mars.2006.0001

Lalich, D. E., Hayes, A. G., & Poggiali, V. (2021). *Explaining bright radar reflections below the Martian south polar layered deposits without liquid water*. eprint.

Lalich, D. E., Hayes, A. G., & Poggiali, V. (2022). Explaining bright radar reflections below the South Pole of Mars without liquid water. *Nature Astronomy*, *6*(10), 1142–1146. https://doi.org/10.1038/s41550-022-01775-z

Lalich, D. E., Holt, J. W., & Smith, I. B. (2019). Radar reflectivity as a proxy for the dust content of individual layers in the Martian North Polar layered deposits. *Journal of Geophysical Research: Planets*, *124*(7), 1690–1703. https://doi.org/10.1029/2018je005787

Landis, M., Dundas, C., McEwen, A., Daubar, I., Hayne, P., Byrne, S., et al. (2024). New, dated small impacts on the south polar layered deposits (SPLD), Mars, and implications for shallow subsurface properties. *Icarus*, 115977. https://doi.org/10.1016/j.icarus.2024.115977

Landis, M. E., & Whitten, J. L. (2022). Geologic context of the bright MARSIS reflectors in Ultimi Scopuli, south polar layered deposits, Mars. *Geophysical Research Letters*, *49*(10), e2022GL098724. https://doi.org/10.1029/2022gl098724

Lauro, S., Orosei, C., Cartacci, M., Cicchetti, A., Cartacci, M., Mattei, E., et al. (2019). Liquid water detection under the south polar layered deposits of Mars—A probabilistic inversion approach. *Remote Sensing*, *11*(20), 2445. https://doi.org/10.3390/rs11202445

Lauro, S. E., Pettinelli, E., Caprarelli, G., Baniamerian, J., Mattei, E., Cosciotti, B., et al. (2022). Using MARSIS signal attenuation to assess the presence of South Polar Layered Deposit subglacial brines. *Nature Communications*, *13*(1), 5686. https://doi.org/10.1038/s41467-022-33389-4

Lauro, S. E., Pettinelli, E., Caprarelli, G., Guallini, L., Rossi, A. P., Mattei, E., et al. (2020). Multiple subglacial water bodies below the South Pole of Mars unveiled by new MARSIS data. *Nature Astronomy*, *5*(1), 63–70. https://doi.org/10.1038/s41550-020-1200-6

Looyenga, H. (1965). Dielectric constants of heterogeneous mixtures. *Physica*, *31*(3), 401–406. https://doi.org/10.1016/0031-8914(65)90045-5

Mattei, E., Pettinelli, E., Lauro, S. E., Stillman, D. E., Cosciotti, B., Marinangeli, L., et al. (2022). Assessing the role of clay and salts on the origin of MARSIS basal bright reflections. *Earth and Planetary Science Letters*, *579*, 117370. https://doi.org/10.1016/j.epsl.2022.117370

Mouginot, J., Kofman, W., Safaeinili, A., Grima, C., Herique, A., & Plaut, J. (2009). MARSIS surface reflectivity of the south residual cap of Mars. *Icarus*, *201*(2), 454–459. https://doi.org/10.1016/j.icarus.2009.01.009

Mouginot, J., Pommerol, A., Kofman, W., Beck, P., Schmitt, B., Herique, A., et al. (2010). The 3–5MHz global reflectivity map of Mars by MARSIS/Mars Express: Implications for the current inventory of subsurface H2O. *Icarus*, *210*(2), 612–625. https://doi.org/10.1016/j.icarus.2010.07.003

Ojha, L., Buffo, J., & Journaux, B. (2024). Thermophysical arguments against basal melting in the south polar region of Mars. *Icarus*, *407*, 115772. https://doi.org/10.1016/j.icarus.2023.115772

Ojha, L., Karimi, S., Buffo, J., Nerozzi, S., Holt, J. W., Smrekar, S., & Chevrier, V. (2021). Martian Mantle heat flow estimate from the lack of lithospheric flexure in the South Pole of Mars: Implications for planetary evolution and basal melting. *Geophysical Research Letters*, *48*(2). e2020GL091409. https://doi.org/10.1029/2020gl091409

Orosei, R., Caprarelli, G., Lauro, S., Pettinelli, E., Cartacci, M., Cicchetti, A., et al. (2022). Numerical simulations of radar echoes rule out basal CO2 ice deposits at Ultimi Scopuli, Mars. *Icarus*, *386*, 115163. https://doi.org/10.1016/j.icarus.2022.115163

Orosei, R., Ding, C., Fa, W., Giannopoulos, A., Hérique, A., Kofman, W., et al. (2020). The global search for liquid water on Mars from orbit: Current and future perspectives. *The Life*, *10*(8), 120. https://doi.org/10.3390/life10080120

Orosei, R., Lauro, S. E., Pettinelli, E., Cicchetti, A., Coradini, M., Cosciotti, B., et al. (2018). Radar evidence of subglacial liquid water on Mars. *Science*, *361*(6401), 490–493. https://doi.org/10.1126/science.aar7268

Picardi, G., Plaut, J. J., Biccari, D., Bombaci, O., Calabrese, D., Cartacci, M., et al. (2005). Radar soundings of the subsurface of Mars. *Science*, *310*(5756), 1925–1928. https://doi.org/10.1126/science.1122165

Plaut, J. J., Picardi, G., Safaeinili, A., Ivanov, A. B., Milkovich, S. M., Cicchetti, A., et al. (2007). Subsurface radar sounding of the south polar layered deposits of Mars. *Science*, *316*(5821), 92–95. https://doi.org/10.1126/science.1139672

Rust, A., Russell, J., & Knight, R. (1999). Dielectric constant as a predictor of porosity in dry volcanic rocks. *Journal of Volcanology and Geothermal Research*, *91*(1), 79–96. https://doi.org/10.1016/s0377-0273(99)00055-4

Seu, R., Phillips, R. J., Biccari, D., Orosei, R., Masdea, A., Picardi, G., et al. (2007). SHARAD sounding radar on the Mars reconnaissance orbiter. *Journal of Geophysical Research*, *112*(E5). https://doi.org/10.1029/2006je002745

Smith, I. B., Lalich, D. E., Rezza, C., Horgan, B. H. N., Whitten, J. L., Nerozzi, S., & Holt, J. W. (2021). A solid interpretation of bright radar reflectors under the Mars South Polar ice. *Geophysical Research Letters*, *48*(15). https://doi.org/10.1029/2021gl093618

Smith, P. H., Tamppari, L. K., Arvidson, R. E., Bass, D., Blaney, D., Boynton, W. V., et al. (2009). H_2O at the Phoenix landing site. *Science*, *325*(5936), 58–61. https://doi.org/10.1126/science.1172339

Sori, M. M., & Bramson, A. M. (2019). Water on Mars, with a grain of salt: Local heat anomalies are required for basal melting of ice at the South Pole today. *Geophysical Research Letters*, *46*(3), 1222–1231. https://doi.org/10.1029/2018gl080985

Stillman, D., & Olhoeft, G. (2008). Frequency and temperature dependence in electromagnetic properties of Martian analog minerals. *Journal of Geophysical Research*, *113*(E9), 9005. https://doi.org/10.1029/2007JE002977

Stillman, D., Pettinelli, E., Lauro, S., Mattei, E., Caprarelli, G., Cosciotti, B., et al. (2022). Partially-Saturated brines within basal ice or sediments can explain the bright basal reflections in the south polar layered deposits. *Journal of Geophysical Research: Planets*, *127*(10), e2022JE007398. https://doi.org/10.1029/2022je007398

Telford, W. M., Gedart, L. P., & Sheriff, R. E. (1990). *Applied geophysics*, (2nd). Cambridge University Press.

Tulaczyk, S. M., & Foley, N. T. (2020). The role of electrical conductivity in radar wave reflection from glacier beds. *The Cryosphere*, *14*(12), 4495–4506. https://doi.org/10.5194/tc-14-4495-2020

Ulaby, F. T. (2014). *Fundamentals of applied electromagnetics* (7th ed.). Prentice Hall.

Whitten, J. L., & Campbell, B. A. (2018). Lateral continuity of layering in the Mars south polar layered deposits from SHARAD sounding data. *Journal of Geophysical Research: Planets*, *123*(6), 1541–1554. https://doi.org/10.1029/2018je005578

Yeh, P. (1998). *Optical waves in layered media*. John Wiley and Sons, Inc.

Zuber, M. T., Phillips, R. J., Andrews Hanna, J. C., Asmar, S. W., Konopliv, A. S., Lemoine, F. G., et al. (2007). Density of Mars' south polar layered deposits. *Science*, *317*(5845), 1718–1719. https://doi.org/10.1126/science.1146995